[CANCER RESEARCH 64, 152–161, January 1, 2004]

Tumor Cell-Derived Nitric Oxide Is Involved in the Immune-Rejection of an Immunogenic Murine Lymphoma

De-En Hu,[1] Stephanie O. M. Dyke,[1] Alistair M. Moore,[1] Lindy L. Thomsen,[2] and Kevin M. Brindle[1]

[1]Department of Biochemistry, University of Cambridge, Cambridge, and [2]Immunomodulation Section, Immunotherapeutics Department, GlaxoSmithKline, Stevenage, United Kingdom

ABSTRACT

The roles played by host-derived nitric oxide (NO) in the growth and subsequent immune rejection of a immunogenic murine lymphoma were investigated by growing the tumor in mice in which the gene for either inducible NO synthase (iNOS) or endothelial NOS (eNOS) had been ablated. This showed that NO from tumor-infiltrating host cells had no significant effect on either tumor growth or immune rejection, although measurements of tumor nitrite levels and protein nitration showed that there had been significant NO production in the rejected tumors, in both the eNOS and iNOS knockout mice. Inhibition of both tumor and host NOS activities, with an iNOS-selective inhibitor (1400W), a nonselective NOS inhibitor [*Nω*-nitro-L-arginine methyl ester (L-NAME)], or scavenging NO with a ruthenium-based scavenger, significantly delayed tumor rejection, while having no appreciable effect on tumor growth. Incubation of tumor cells with medium taken from cultured splenocytes, that had been isolated from immunized animals and activated by incubating them with irradiated tumor cells, resulted in an increase in tumor cell NOS activity and an increase in tumor cell apoptosis, which could be inhibited using L-NAME. We propose that, during the immune rejection of this tumor model, there is induction of tumor NOS activity by cytokines secreted by activated lymphocytes within the tumor and that this results in increased levels of tumor NO that induce tumor cell apoptosis and facilitate immune rejection of the tumor.

INTRODUCTION

Nitric oxide (NO) mediates a diverse array of biological activities, including vasodilatation, neurotransmission, iron metabolism and immune defense (1). NO is synthesized from L-arginine by the enzyme, NO synthase (NOS), which exists as three isoforms; the two calcium-dependent and constitutive isoforms of NOS, endothelial NOS (eNOS or NOS3) and neuronal NOS (nNOS or NOS1), and the calcium-independent inducible NOS (iNOS or NOS2). The isoforms differ in their capacity to produce NO, with iNOS capable of producing sustained and high concentrations of NO, in the micromolar range, as compared with the pico- to nanomolar concentrations produced by nNOS and eNOS (2). Recent studies have shown that there is also a mitochondrial enzyme, which is a posttranslationally modified form of nNOS (3).

The role of NO in tumor biology is complex and in many respects still poorly understood. There is evidence that NO is involved in both tumor angiogenesis and in immune cell killing of tumor cells and, therefore, can have both positive and negative effects on tumor progression. At relatively low concentrations, NO can protect tumor cells from apoptosis (4, 5), including in the EL-4 cell line used in this study (6), stimulate tumor angiogenesis, and increase tumor blood flow (7, 8), thus promoting tumor growth; whereas at higher levels, it can induce apoptosis and arrest tumor growth (9–11). In tumor cells transfected with vectors expressing iNOS, tumor growth and metastatic potential were shown to be dependent on both the level of NO produced and the presence of wild-type p53 (12–15). Expression of relatively low levels of iNOS caused slower growth of tumors expressing wild-type p53 but faster growth of cells with mutated or no p53. The increased growth of iNOS-expressing tumors was thought to be due to the observed increase in vascularization (12, 14). There is also evidence that low levels of macrophage-derived NO can have a positive effect on tumor vascularization (16), and, indeed, tumor-infiltrating macrophages are known to secrete a number of pro- and antiangiogenic molecules in addition to NO (17, 18). However, expression of higher levels of iNOS caused slow growth and tumor cell death, both *in vitro* and *in vivo*. Early studies showed that activated macrophages, expressing iNOS, could cause cytostasis or cytotoxicity in cocultured tumor cells (19–21) and could be found at high levels in tumors (16, 22). This led to the suggestion that tumor-infiltrating macrophages could provide some form of nonspecific immunity against tumor growth. This was also supported by studies *in vivo*. The inhibition of NO production delayed the rejection of a highly antigenic murine skin tumor (23), and tumor-mediated suppression of macrophage iNOS expression and deletion of the host iNOS gene were both correlated with reduced tumor rejection (24, 25). However, it has been suggested that induction of NO synthesis in the tumors cells themselves could also contribute to tumor rejection (10, 23, 26). The cytokines that induce NO synthesis by tumor-infiltrating macrophages can also induce NO synthesis in tumor cells, resulting in their growth arrest and apoptosis (10, 26).

In this study we have used a combination of selective and nonselective NOS inhibitors, an NO scavenger, and iNOS and eNOS knockout mice to resolve the roles played by host and tumor-cell NOS activity in the growth and subsequent immune rejection of an immunogenic murine lymphoma. These studies have shown that, in this tumor model, host-derived NO has no significant effect on either the growth of the tumor or its subsequent immune rejection. Tumor-derived NO also has no significant effect on tumor growth. However, during immune rejection, increases in tumor cell NOS activity and NO synthesis resulted in increased levels of tumor cell apoptosis and, thus, appear to facilitate the rejection process.

MATERIALS AND METHODS

Cell Lines and Tumor Implantation. The E.G7-OVA cell line was originally derived from the murine thymoma line, EL-4, by transfection with a neomycin-selectable vector expressing full-length chicken ovalbumin (27). The E.G7-OVA and EL-4 cells used in this study were taken from frozen stocks held at GlaxoSmithKline, Stevenage, United Kingdom. The cells were cultured as a suspension in RPMI 1640 (Invitrogen Ltd., Paisley, United Kingdom) containing 10% heat inactivated FCS (PAA Laboratories, GmbH, Linz, Austria), 2 mM L-glutamine, penicillin (100 units/ml), and streptomycin (100 μg/ml). Selection of E.G7-OVA cells was maintained using culture medium containing 400 $\mu g \cdot ml^{-1}$ G418.

Wild-type female C57BL/6 mice were purchased at 6–8 weeks of age from Charles River Ltd. (Thanet, United Kingdom). Female iNOS $^{-/-}$ (28) and eNOS $^{-/-}$ (29) mice were obtained at 6–8 weeks of age from Prof. Salvador

Received 6/19/03; revised 10/27/03; accepted 10/29/03.

Grant support: Grants from the Medical Research Council, United Kingdom, and Cancer Research United Kingdom. Financial support from the Cambridge European Trust, Issac Newton Trust, and the Department of Biochemistry, Cambridge (to S. O. M. D.). Cooperative Award in Science and Engineering studentship from the Biotechnology and Biological Research Council and GlaxoSmithKline (to A. M. M.).

The costs of publication of this article were defrayed in part by the payment of page charges. This article must therefore be hereby marked *advertisement* in accordance with 18 U.S.C. Section 1734 solely to indicate this fact.

Requests for reprints: Kevin M. Brindle, Department of Biochemistry, University of Cambridge, 80 Tennis Court Road, Cambridge CB2 1GA, United Kingdom. Phone: 44-(0)1223-333674; Fax: 44-(0)1223-766002; E-mail: kmb@mol.bio.cam.ac.uk.

Moncada and Dr Adrian Hobbs at the Wolfson Institute, University College London, United Kingdom. Tumor cells (5×10^6) were injected s.c. into the shaved flanks of mice. Tumor size is reported as the product of the two largest perpendicular diameters (mm^2). All of the experiments were conducted in compliance with a project license issued under the Animals (Scientific Procedures) Act 1986 and were designed with reference to the U.K. Co-ordinating Committee on Cancer Research guidelines for the welfare of animals in experimental neoplasia. The work was approved by a local ethical review committee.

Administration of an Selective iNOS Inhibitor (1400W) *in Vivo*. The drug was delivered using a s.c. osmotic minipump (Alzet pump; Charles River Ltd.) with a volume of 200 μl and a delivery rate of 1.0 μl/h. In the treatment groups, the pumps were filled with 50 mg of 1400W in 200 μl of PBS and in the control groups, with PBS alone. 1400W was a generous gift from Glaxo-SmithKline, Stevenage, United Kingdom.

Preparation of an NO Scavenger. A ruthenium(III) polyaminocarboxylate NO scavenger [AMD6221; Ru(H_3dtpa)(Cl)] and its nitrosyl derivative [Ru(H_2dtpa)NO] were prepared as described by Mosi *et al.* (30). The capacities, of the scavenger to bind NO and of the nitrosylated form not to bind NO, were checked by adding them to a freshly prepared solution of NO in water and measuring the change in the free NO concentration using an NO electrode (World Precision Instruments, Inc. Sarasota, FL). For experiments *in vivo* the compounds were dissolved in PBS (pH adjusted to 7.4) and injected i.p. at a dose of 75 mg/kg, twice daily.

Tumor Histology and Immunohistochemistry. Rabbit polyclonal antibodies recognizing CD4, CD8-α, a goat polyclonal antibody recognizing CD68 (M-20), and a secondary antirabbit IgG staining system ("Immuno-Cruz staining system") were purchased from Santa Cruz Biotechnology Inc. Rabbit antihuman Factor VIII antibody was purchased from DAKO, Copenhagen, Denmark, and a rabbit polyclonal antibody to nitrated keyhole limpet hemocyanin was purchased from Upstate Biotechnology, Lake Placid, NY. FITC-conjugated monoclonal antibodies recognizing rabbit and goat IgGs were purchased from Sigma (Gillingham, Dorset, United Kingdom).

Tumors were fixed in fresh 10% formalin and were embedded in paraffin. Five-μm thick sections were cut and stained with H&E (Sigma) or Masson's trichrome stain (Sigma). For immunoperoxidase staining, the rabbit primary antibodies were detected using a biotinylated antirabbit IgG secondary antibody and horseradish peroxidase-conjugated to streptavidin using the Immuno-Cruz staining system, according to the manufacturer's instructions. The slides were lightly counterstained with hematoxylin, light green, or methyl green, depending on the intensity required. For immunofluorescence staining the slides were prepared as for immunoperoxidase staining, except that the peroxidase-block step was omitted. Slides were incubated with an appropriately diluted primary antibody before detection with a fluorescein-conjugated secondary antibody. As a negative control, the sections were treated with nonimmune rabbit serum in place of the primary antibodies, and, in the case of nitrotyrosine detection, the primary antibody was preincubated with either 10 mM nitrotyrosine (Sigma) or 50 μg/ml nitrated BSA in PBS for 1 h at room temperature. Nitrated BSA was prepared by incubating BSA (6 mg/ml) for 18 h at room temperature with 10 mM $NaNO_2$, 0.3% H_2O_2, and 9 μM $FeCl_3$. The protein was subsequently precipitated with four volumes of ethanol (31).

Flow cytometry was also performed on cell suspensions prepared from tumor tissue and on the tumor cells grown in culture. Flow cytometry was performed using a FACScan Instrument and analyzed with Lysys II software (Becton Dickinson, Mountain View, CA). Tumor cell suspensions were prepared from tumor tissue by grinding the excised tumor through a stainless steel mesh (32) into serum-free RPMI 1640.

Tumor vascular volumes were analyzed using an axial strip sampling technique (33). Sections stained with Masson's trichrome stain or with antibody to Factor VIII were examined at $\times$200, and the images were relayed to a computer. The volume fraction occupied by the blood vessels was estimated using a 486-point square lattice (18×27) with a field-of-view of 0.209 mm^2. Functional vessels were determined in a similar manner after i.v. injection of carmine red dye (Sigma; Refs. 34, 35). The tumors were then excised postmortem and were fixed in a solution of 10% formalin in saline. Sections (5 μm thick) from the fixed and paraffin-embedded tumors were then cut, deparaffinized, and counterstained in 2% light green dye (Sigma).

Selection of E.G7-OVA Cell Clones Expressing High Levels of Surface Ovalbumin. A parent population of E.G7-OVA cells at nominal passage 6 was recloned by limiting dilution in RPMI 1640 containing 10% heat-inactivated FCS. Approximately 5×10^7 cells of each clone were stained for surface ovalbumin using a rabbit anti-ovalbumin primary antibody (Europa) and a FITC-conjugated monoclonal antirabbit immunoglobulin secondary antibody (Sigma). Fluorescence was analyzed using a Coulter XL flow cytometer and Expo 32 acquisition and analysis software (BeckmanCoulter). A clone expressing relatively high levels of surface ovalbumin was selected for additional studies.

NOS Activities in Cell and Tumor Extracts. Tumor tissue was homogenized using an Omni GLH-220 homogenizer [Omni International, Inc. Warrenton, VA; 1 g of tissue in 2.5 ml of ice-cold buffer containing 250 mM Tri-HCl (pH 7.4), 10 mM EDTA, 10 mM EGTA, and 1 ml/50 ml of a protease inhibitor mixture (Sigma)] and was centrifuged at 16,000 $\times$ *g*, and the supernatants were passed through 0.45 μm Millex filters (Millipore Corporation, Bedford, MA) and were assayed for NOS activity after the conversion of [^{14}C]-L-arginine (Amersham, Arlington Heights, IL) to [^{14}C]citrulline. The supernatants (10 μl) were added to 40 μl of an assay mixture containing 33 mM Tris-HCl (pH 7.4), 4 μM tetrahydrobiopterin, 1 μM flavin adenine dinucleotide, 1 μM flavin adenine mononucleotide, 1.25 mM NADPH, 0.05 μCi [^{14}C]arginine, and 0.75 mM $CaCl_2$. Reactions were incubated at room temperature (23°C) for 30 min and were terminated by adding 450 μl of a stop buffer containing 50 mM HEPES (pH 5.5) and 5 mM EDTA. The reaction mixtures were then applied immediately to columns containing 0.8 ml of Dowex ion exchange resin 50WX8 (200–400 mesh in the H^+ form; SUPELCO, Bellefonte, PA). [^{14}C]Citrulline was collected in the flow-through fraction and was mixed with scintillation fluid, and radioactivity was counted in a Beckman LS 3801 liquid scintillation counter. Protein content of the tumor homogenates was determined spectrophotometrically with Bradford's reagent (Bio-Rad), using BSA as standard. NOS activity is expressed as pmol of citrulline per minute per milligram of protein. For measurements of NOS activity in cultured tumor cells, the cells were harvested from a growing culture and washed in ice-cold PBS; and then, $\sim 2 \times 10^8$ cells were resuspended in 25 ml of fresh extraction buffer in a tight-fitting Potter homogenizer. The buffer contained 50 mM Tris-HCl (pH 8.2), 2 mM DTT, 2 mM EDTA, and 1% Triton X-100. After 10 strokes with the pestle, the resulting cell extracts were kept on ice for 30 min and then were centrifuged for 15 min at 2000 $\times$ *g*, to remove any insoluble material. The supernatants were removed and were assayed immediately.

Determination of Nitrite Concentration. NO production was determined by measuring the accumulation of nitrite, assayed using either Griess reagent (2) or a fluorometric assay based on the reaction of nitrite with 2,3-diaminonaphthalene (36). Nitrite concentrations were determined in cell culture supernatants and in tumor homogenates that were prepared as described above. All of the samples were passed through a M_r 10,000 ultrafiltration membrane before assay (Ref. 36; Vivascience, Goettingen, Germany). Sodium nitrite was used as a standard.

Splenocyte Restimulation *in Vitro* and Production of Conditioned Medium. Collection of splenocytes and their restimulation *in vitro* were performed essentially as described by Ju *et al.* (37) and Ke *et al.* (38). Spleens were collected from mice that had been effectively immunized against ovalbumin by implanting them with E.G7-OVA tumor cell clones that expressed relatively high levels of surface ovalbumin (see "Results"). The spleens were collected 30 days after immune rejection of the tumor and were washed in RPMI 1640 culture medium, and the splenocytes were released by mechanical dissociation. Cells from five spleens were harvested by centrifugation, incubated for 1 min on ice in a red cell lysis buffer (154 mM NH_4Cl, 10 mM $KHCO_3$, and 0.15 mM EDTA), and then resuspended in fresh culture medium. The cells were restimulated by coculturing them with E.G7-OVA cells that had been X-irradiated at a density of 10^7 cells/ml with 20,000 Rads. For production of conditioned medium, a splenocyte suspension (25 ml at a density of 2×10^6 cells/ml) was cocultured with the irradiated E.G7-OVA cells (5 ml at a density of 2×10^6 cells/ml) for 7 days, and the culture medium was collected. Splenocytes that were collected from animals implanted with EL-4 tumors and that had been incubated with irradiated EL-4 cells were used to produce a conditioned medium control.

To determine the effect of splenocyte-conditioned medium on EL-4 cells, the cells were cultured in a 50/50 mixture of the conditioned medium with

fresh RPMI 1640, and the levels of apoptosis, NOS activities, and nitrite concentrations were determined after 0, 24, and 48 h of incubation.

Measurement of Apoptosis. Apoptosis was scored by monitoring nuclear fragmentation after cell staining with 50 μg/ml propidium iodide and 10 μg/ml acridine orange. Cells that possessed condensed or fragmented nuclei but intact plasma membranes were scored as apoptotic (39). Alternatively, apoptosis was determined using the Vybrant Apoptosis Assay Kit (Molecular Probes, Inc, Eugene, OR). After staining a cell population with FITC-labeled annexin V and propidium iodide, the stained cells were analyzed by flow cytometry, measuring the fluorescence emission at 530 nm and >575 nm.

RESULTS

The E.G7-OVA cell line, which was derived from the H-2^b lymphoma EL-4 by transfection with a vector expressing chicken ovalbumin (27), has been widely used in studies of immune responses to tumor cells (32, 40–43). We showed previously (35) that the tumorigenicity of this cell line was dependent on its nominal passage number, with early passage cells showing significantly higher levels of spontaneous immune rejection than late passage cells. The incidence of rejection appeared to correlate with the surface expression of ovalbumin determined using flow cytometry, with later passage cells showing lower levels of expression (35). In the later stages of the present study, we recloned some early-passage cells (nominal passage 6) and then selected clones expressing relatively high levels of surface ovalbumin (see "Materials and Methods" section). Throughout this study, we have used, in addition to the untransfected EL-4 cell line, this recloned cell line, which expressed relatively high levels of surface ovalbumin and which formed tumors that always underwent spontaneous regression, and the lower expressers used in our previous study (35), which showed variable levels of spontaneous regression. That the regression of tumors expressing high levels of surface ovalbumin was due to immune rejection was confirmed by demonstrating the unrestricted growth of a high-expressing tumor in a severe combined immunodeficient mouse (Fig. 1*D*). Because the growth of tumors was dependent on the nominal passage number of the E.G7-OVA cell lines, and could also depend on the conditions under which the EL-4 and E.G7-OVA cell lines had been cultured and the age of the animals, it made it difficult to compare the results obtained between different tumor cell implantations. For these reasons, results were compared only between tumors implanted at the same time and from the same batch of cultured tumor cells (individual panels shown in Fig. 1).

To investigate the role of host-derived NO in the growth and immune rejection of E.G7-OVA tumors, EL-4 cells, early- and late-

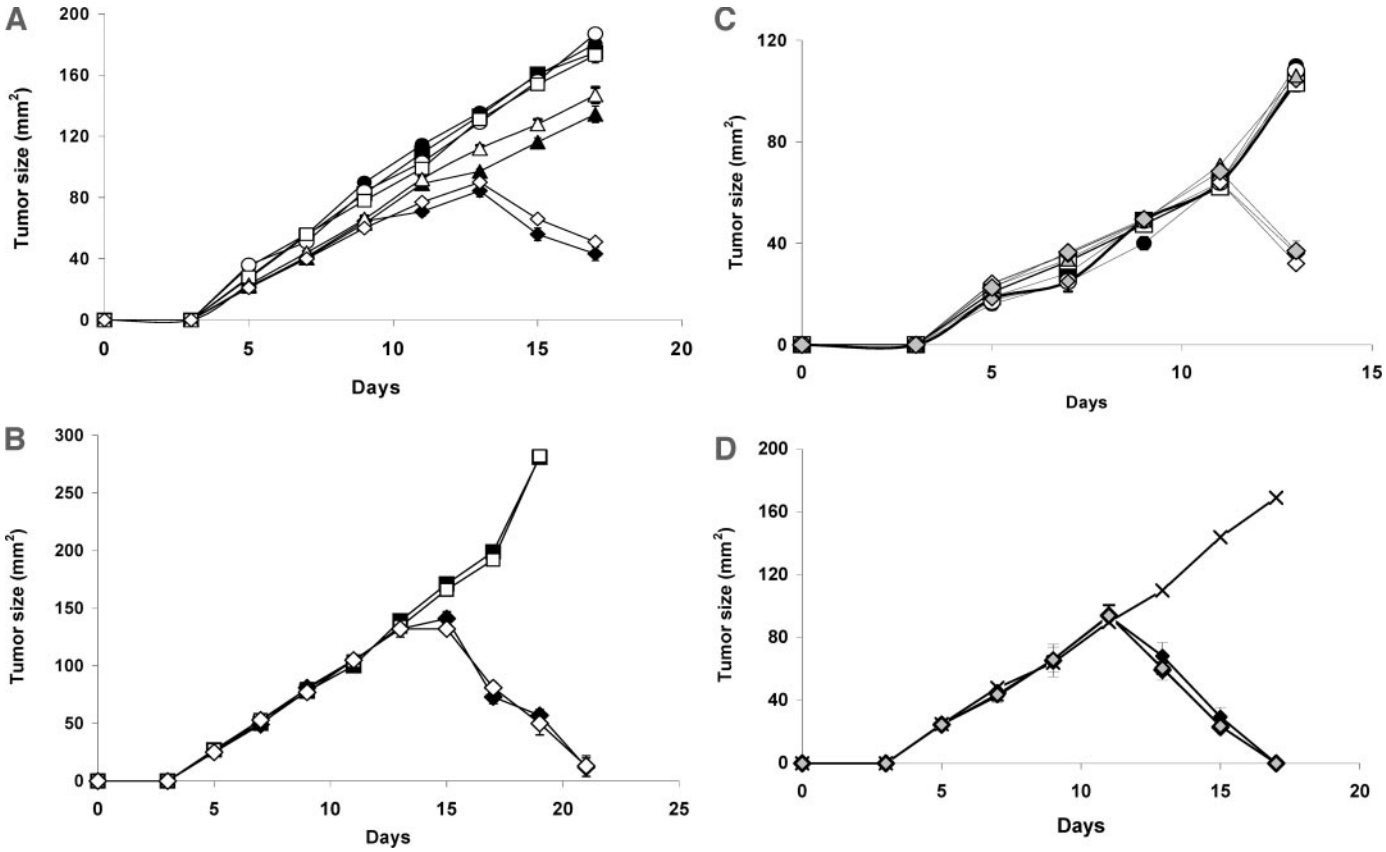

Fig. 1. Growth of implanted tumors in wild-type (*filled symbols*) and in inducible nitric oxide synthase (iNOS; *open symbols*) and endothelial nitric oxide synthase (eNOS; *gray symbols*) knockout mice. *Data points*, means ± SE of the volumes reported as the product of the two largest perpendicular diameters. Where the error bars are not visible they lie within the symbol. Tumors were implanted by s.c. injection of 5×10^6 cells at $t = 0$ days. *A*, the growth rates of the EL-4 and progressive E.G7.OVA tumors were significantly less than those of the E.G7.OVA tumors that went on to regress ($P < 0.001$, ANOVA). Wild-type mice implanted with: EL-4 tumors ($n = 9$; ●); E.G7-OVA tumors, arising from cells implanted at nominal passage number 14 ($n = 9$; ■); E.G7-OVA tumors, arising from cells implanted at nominal passage number 9 ($n = 9$; ▲); regressive E.G7-OVA tumors (four arising from cells implanted at nominal passage number 9 and 2 arising from cells implanted at nominal passage number 14; ◆). iNOS knockout mice implanted with: EL-4 tumors ($n = 8$; ○); E.G7-OVA tumors, arising from cells implanted at nominal passage number 14 ($n = 8$; □); E.G7-OVA tumors arising from cells implanted at nominal passage number 9 ($n = 6$; △); regressive E.G7-OVA tumors (2 arising from cells implanted at nominal passage number 14 and 2 arising from cells implanted at nominal passage number 9; ◇). *B*, wild-type mice implanted with: E.G7-OVA tumors ($n = 14$; ■); regressive E.G7-OVA tumors ($n = 2$; ◆). iNOS knockout mice implanted with: E.G7-OVA tumors ($n = 14$; □); regressive E.G7-OVA tumors ($n = 2$; ◇). All of the tumors arose from cells implanted at nominal passage number 12. *C*, wild-type mice implanted with EL-4 tumors ($n = 3$; ●); E.G7-OVA tumors, ($n = 9$; ■); regressive E.G7-OVA tumors ($n = 3$; ◆). iNOS knockout mice implanted with EL-4 tumors ($n = 3$; ○); E.G7-OVA tumors, ($n = 9$; □); regressive E.G7-OVA tumors ($n = 3$; ◇). eNOS knockout mice implanted with: EL-4 tumors ($n = 3$; ◍); E.G7-OVA tumors, ($n = 9$; ▣); regressive E.G7-OVA tumors ($n = 3$; ◈). All of the tumors arose from cells implanted at nominal passage number 8. *D*, regressive E.G7-OVA tumors arising from the recloned cells expressing high levels of surface ovalbumin in: severe combined immunodeficient mice ($n = 1$; ×); wild-type mice ($n = 7$; ◆); iNOS knockout mice ($n = 6$; ◇); eNOS knockout mice ($n = 6$; ◈).

passage E.G7-OVA cells, and the recloned E.G7-OVA cells, expressing relatively high levels of surface ovalbumin, were implanted in wild-type mice and in eNOS and iNOS knockout mice (Fig. 1). Removal of either host iNOS or host eNOS activity had no significant effect on the growth of EL-4 tumors or on the growth and rejection of E.G7-OVA tumors. Each panel in Fig. 1 represents a separate, independent experiment. Previous studies have shown that there is a significant increase in immune cell infiltration in those tumors that express ovalbumin and that this increase is even greater in those tumors undergoing immune rejection (32, 35, 41). This was confirmed in the present study by both flow cytometric (Table 1A) and immunohistochemical analyses (Table 1B) of EL-4 and E.G7-OVA tumors. E.G7-OVA tumors undergoing regression showed significantly higher levels of cells expressing CD4, CD8, and CD68 when compared with EL-4 tumors. CD68 is a macrophage antigen (44). However, this increased immune cell infiltration was unaffected by host NOS status, being the same in iNOS and eNOS knockout and wild-type mice. We have shown previously (35) that immune rejection in this tumor model is accompanied by vascular proliferation, a feature that has been observed in other tumors undergoing immune rejection. This, too, was unaffected by host NOS status. The vascular volumes in regressing E.G7-OVA tumors were significantly higher than in EL-4 tumors, regardless of whether the tumors were growing in eNOS or iNOS knockout or wild-type mice (Fig. 2).

The lack of any detectable effect of host NOS activity on the immune rejection of E.G7-OVA tumors suggested that the production of NO might play no role in the immune rejection of this particular tumor type. Therefore, we sought evidence for the production of NO and of the cellular damage that relatively high levels of NO can cause. The production of NO in the tumors was assessed by measuring the concentration of accumulated nitrite, which is formed from NO by oxidation (2). Cellular damage resulting from NO production was assessed by measuring the levels of nitrotyrosine, which is formed after the interaction of NO or NO-derived secondary products with reactive oxygen species (ROS; Refs. 45, 46). The latter, like NO, can be produced at relatively high levels by macrophages. Nitrite accumulation and nitrotyrosine staining were significantly increased in progressive E.G7-OVA tumors when compared with EL-4 tumors, and both were further increased in regressive E.G7-OVA tumors (Figs. 3 and 4). However, the levels of tumor nitrite accumulation and nitrotyrosine staining were unaffected by host NOS status, the levels being the same, for each tumor type, in the iNOS knockout, the eNOS knockout, and the wild-type mice.

Table 1 *Immune cell infiltration in EL-4 and regressive E.G7-OVA tumors in wild-type and in iNOS and eNOS knockout mice*

	Control	CD8	CD4	CD68
A. Flow cytometric analysis[a]				
EL-4 (wild-type)	4.5 ± 0.3	82.2 ± 7.1	52.3 ± 7.7	37.7 ± 5.3
E.G7-OVA (wild-type)	4.1 ± 0.3	155.3 ± 7.4[b]	119.5 ± 5.8[b]	101.1 ± 6.3[b]
E.G7-OVA (iNOS k.o.)	3.8 ± 0.2	138.1 ± 6.6[b]	129.6 ± 6.6[b]	100.9 ± 6.3[b]
B. Immunohistochemical analysis[c]				
EL-4 (wild-type)		10.9 ± 0.8	28.4 ± 0.7	7.5 ± 1.0
E.G7-OVA (wild-type)		76.5 ± 1.8[b]	73.3 ± 1.7[b]	60.0 ± 3.6[b]
EL-4 (iNOS k.o.)		9.7 ± 1.8	30.0 ± 2.9	6.3 ± 2.4
E.G7-OVA (iNOS k.o.)		73.6 ± 1.9[b]	78.9 ± 4.1[b]	58.4 ± 4.2[b]
EL-4 (eNOS k.o.)		8.8 ± 1.4	27.3 ± 1.5	8.4 ± 1.3
E.G7-OVA (eNOS k.o.)		75.5 ± 1.8[b]	75.3 ± 1.6[b]	60.0 ± 2.1[b]

[a] Flow cytometric analysis of cell suspensions prepared by mechanical disaggregation of tumors excised 13 days after implantation. Three tumors were used in each group and the numbers represent the mean ± SE of the fluorescence intensities in arbitrary units. The control data were obtained in the absence of the primary antibody.

[b] Significantly different from the EL-4 tumor in wild-type mice ($P < 0.01$).

[c] Immunohistochemical analysis of tumor sections. The number of staining cells in 15 high power (×200) fields-of-view are given (mean ± SE). There were three mice in each group.

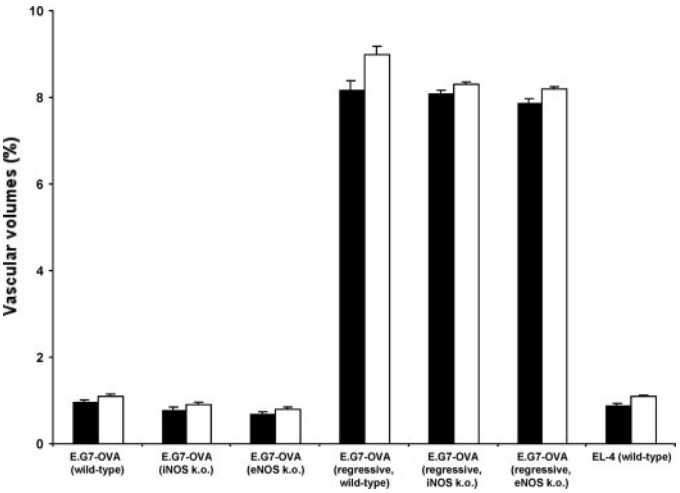

Fig. 2. Vascular volumes in EL-4, progressive E.G7-OVA and regressive E.G7-OVA tumors in wild-type, inducible nitric oxide synthase knockout (*iNOS k.o.*), and endothelial nitric oxide synthase knockout (*eNOS k.o.*) mice. Tumors were excised 13 days after implantation. Vascular volumes are given as the mean percentage volume ± SE for 30 different tumor areas stained with Masson's trichrome stain (■) or from carmine dye-injected tumors (□). Three tumors were used in each group. Vascular volumes in regressive E.G7-OVA tumors were significantly higher than in the EL-4 or in the progressive E.G7-OVA tumors ($P < 0.01$).

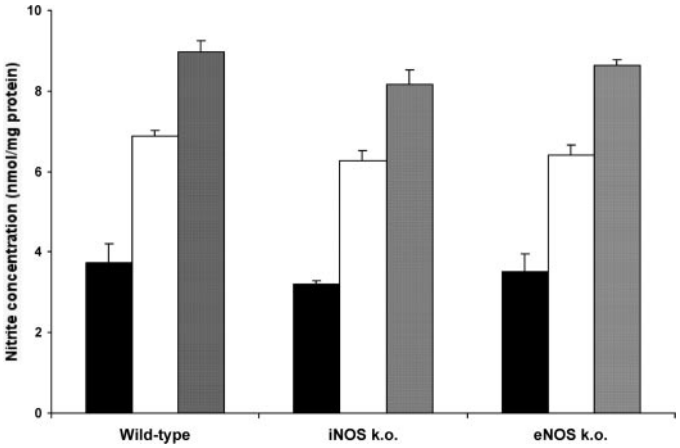

Fig. 3. Nitrite concentrations in EL-4, progressive E.G7-OVA, and regressive E.G7-OVA tumors in wild-type, inducible nitric oxide synthase knockout (*iNOS k.o.*), and endothelial nitric oxide synthase knockout (*eNOS k.o.*) mice. Tumors were excised 13 days after implantation and were homogenized, and the nitrite concentration determined using Griess reagent. The nitrite concentration is given as the mean (nmol/mg protein) ± SE in EL-4 tumors (■, $n = 3$ in wild-type, iNOS k.o. and eNOS k.o. mice); progressive E.G7-OVA tumors (□, $n = 17$ in wild-type and iNOS k.o. mice and $n = 5$ in eNOS k.o. mice), and regressive E.G7-OVA tumors (▩, $n = 6$ in wild-type mice and $n = 4$ in iNOS k.o. and eNOS k.o. mice). The nitrite concentration was significantly higher in regressive and progressive E.G7-OVA tumors when compared with EL-4 tumors ($P < 0.01$).

The presence of increased levels of nitrite and nitrotyrosine staining in regressing E.G7-OVA tumors suggested that NO might be playing a role in tumor immune rejection; however, the absence of any effect of host NOS status implied that this NO must be coming from the tumor cells themselves. We confirmed that this was possible by measuring iNOS and eNOS activities in EL-4, in progressive E.G7-OVA, and in regressive E.G7-OVA tumors taken from iNOS knockout, eNOS knockout, and wild-type mice (see Fig. 5). The activities shown were those obtained after subtraction of the NADPH-independent activity, which was substantial in both the tumor and liver samples at between 60 and 80% of the total measured activity. The contribution of the different NOS isoforms to the measured NOS activity was determined by using W13 (200 μM) as a selective inhibitor of the

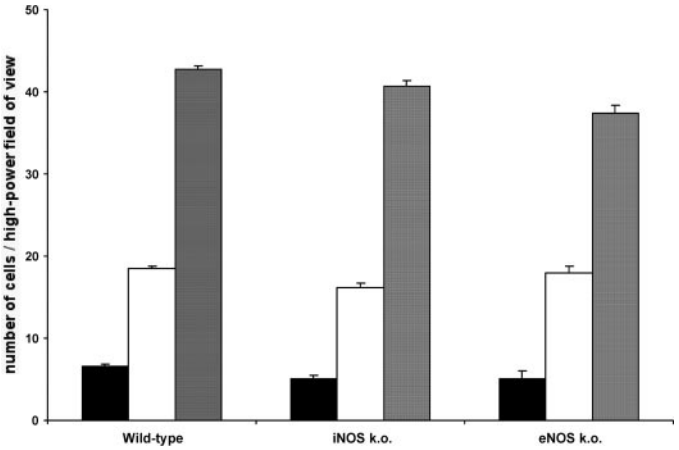

Fig. 4. Nitrotyrosine staining in EL-4, progressive E.G7-OVA, and regressive E.G7-OVA tumors in wild-type, inducible nitric oxide synthase knockout (*iNOS k.o.*) and endothelial nitric oxide synthase knockout (*eNOS k.o.*) mice. Data shown are the mean ± SE of the number of cells in 15 high-power (×200) fields-of-view. Three tumors were used in each group. EL-4 tumors (■), progressive E.G7-OVA tumors (□) and regressive E.G7-OVA tumors (▨). Staining was significantly higher in progressive and regressive E.G7-OVA tumors when compared with EL-4 tumors ($P < 0.01$).

calcium-dependent isoforms (eNOS and nNOS; Ref. 2) and 1400W [*N*-(3-aminomethyl)benzylacetamide-2HCl] (100 nM) as a selective inhibitor of the calcium-independent isoform (iNOS; Ref. 47). These measurements showed that there were substantial activities of both the calcium-dependent and the calcium-independent NOS isoforms in extracts of EL-4 and E.G7-OVA tumors and that the total NOS activity was significantly higher ($P < 0.01$, ANOVA) in the E.G7-OVA tumors than in the EL-4 tumors. Furthermore, measurements of NOS activity in tumors taken from the eNOS and iNOS knockout mice demonstrated that most of this NOS activity must have been in the tumor cells, as opposed to host cells present in the tumor, such as infiltrating immune cells and endothelial cells. The presence of eNOS, nNOS, and iNOS in EL-4 cells has also been demonstrated by Western blotting (6). Measurements on liver extracts, in the presence of the isoform-selective inhibitors, confirmed the NOS status of the eNOS and iNOS knockout mice (Fig. 5). The NOS activities measured in the regressive E.G7-OVA tumors were less than those measured in the growing tumors and reflect presumably the loss of tumor cells and deposition of collagen that we have observed previously after the onset of regression in this tumor model (35).

Because the majority of tumor NOS activity was present in the tumor cells, we investigated the effect of inhibiting tumor NO production on tumor growth and subsequent immune rejection. Administration of *N*ω-nitro-L-arginine methyl ester (L-NAME) in the drinking water, a nonspecific NOS inhibitor (2), resulted in significant inhibition of tumor NOS activity, reducing both the nitrite content and protein nitration of E.G7-OVA tumors. The nitrite content was 6.2 ± 0.2 nmol/mg protein in the treated group *versus* 10.9 ± 0.5 nmol/mg protein ($n = 3$; mean ± SE; $P < 0.01$) in the control group. Protein nitration, assessed using an antinitrotyrosine antibody and expressed as the number of staining cells in 10 high-power (×200) fields-of-view, was 6.5 ± 0.4 in the treated group *versus* 12.5 ± 0.3 ($n = 3$; 10 sections; mean ± SE; $P < 0.01$) in the controls. The tumors were derived from the recloned E.G7-OVA cells expressing high levels of surface ovalbumin and were excised for these measurements at 13–15 days after implantation. The inhibition of tumor NOS activity with L-NAME had no significant effect on the growth of E.G7-OVA tumors derived from cells expressing relatively low levels of ovalbumin on their surface (nominal cell passage number 23; data not shown). However, it delayed significantly the regression of E.G7-OVA tumors derived from the recloned E.G7-OVA cell line expressing higher levels of surface ovalbumin (Fig. 6*A*). A similar result was obtained after s.c. administration of the iNOS-selective inhibitor, 1400W (Fig. 6*B*). L-NAME and 1400W also appeared to inhibit slightly the growth of the E.G7-OVA cells expressing high levels of ovalbumin (Fig. 6, *A* and *B*), however this was not statistically significant. The tumor sizes measured in the first 12 days after tumor implantation were not significantly different between the control and drug-treated groups ($P > 0.05$, ANOVA). Administration of a ruthenium-based NO scavenger (30), which has been shown previously to delay cardiac allograft rejection (48), also delayed rejection of E.G7-OVA tumors, while having no significant effect on their growth (Fig. 6*C*). The tumor sizes measured after 12 days for the L-NAME-, 1400W-, and NO scavenger-treated animals were significantly larger than those in the control groups ($P < 0.01$, ANOVA). The nitrosylated scavenger (see "Materials and Methods" section) had no effect on either tumor growth or rejection. Three paired experiments were performed with the scavenger and the nitrosylated scavenger as a control (data not shown).

These studies had clearly demonstrated a role for tumor-derived NO in the immune rejection of E.G7-OVA tumors, although the mechanism(s) by which it had promoted tumor rejection were not clear. Histological analysis of regressing E.G7-OVA tumors showed an association of nitrotyrosine staining with the presence of apoptotic tumor cells, as has been observed previously (Ref. 45; Fig. 7). Apoptotic cells were readily observable in H&E-stained and Masson's

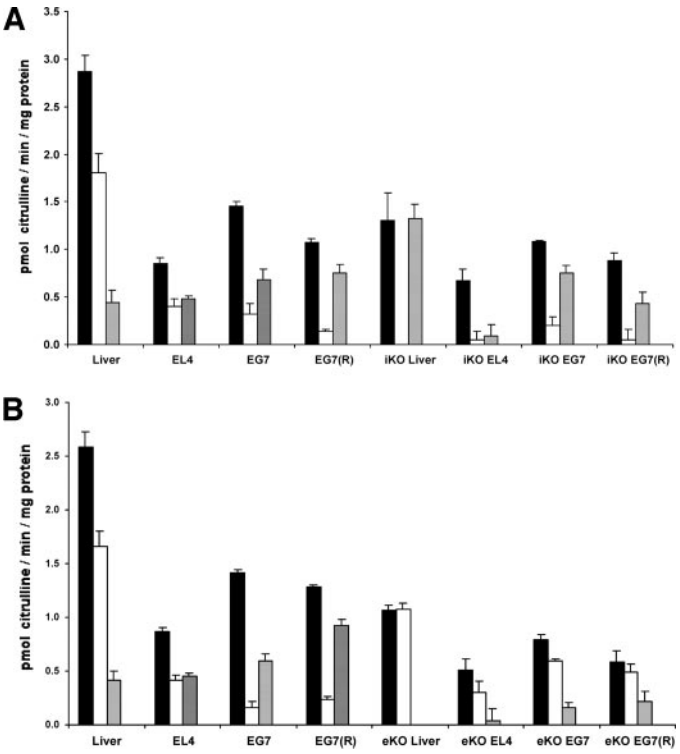

Fig. 5. Nitric oxide synthase (NOS) activity measured in tumor extracts prepared from wild-type, inducible NOS (iNOS) knockout, and endothelial NOS (eNOS) knockout mice. The activities shown were those obtained after subtraction of the activities measured in the absence of NADPH. ■, total NOS activity; □, NOS activity measured in the presence of the constitutive isoform(s) of NOS (cNOS) inhibitor, W13 (200 μM), (*i.e.*, iNOS activity); ▨, the activity measured in the presence of the iNOS inhibitor, 1400W (100 nM), (*i.e.*, cNOS activity). *A*, NOS activities measured in extracts of EL-4 (*EL4*), progressive E.G7-OVA (*EG7*), and regressing E.G7-OVA [*EG7(R)*] tumors in wild-type and iNOS knockout (*iKO*) mice. *B*, NOS activities measured in extracts of EL-4 (EL4), progressive E.G7-OVA (*EG7*), and regressing E.G7-OVA [*EG7(R)*] tumors in wild-type and eNOS knockout (*eKO*) mice. There was a higher total NOS activity in E.G7-OVA tumors compared with EL-4 tumors in wild-type, iKO and eKO mice ($P < 0.01$, ANOVA).

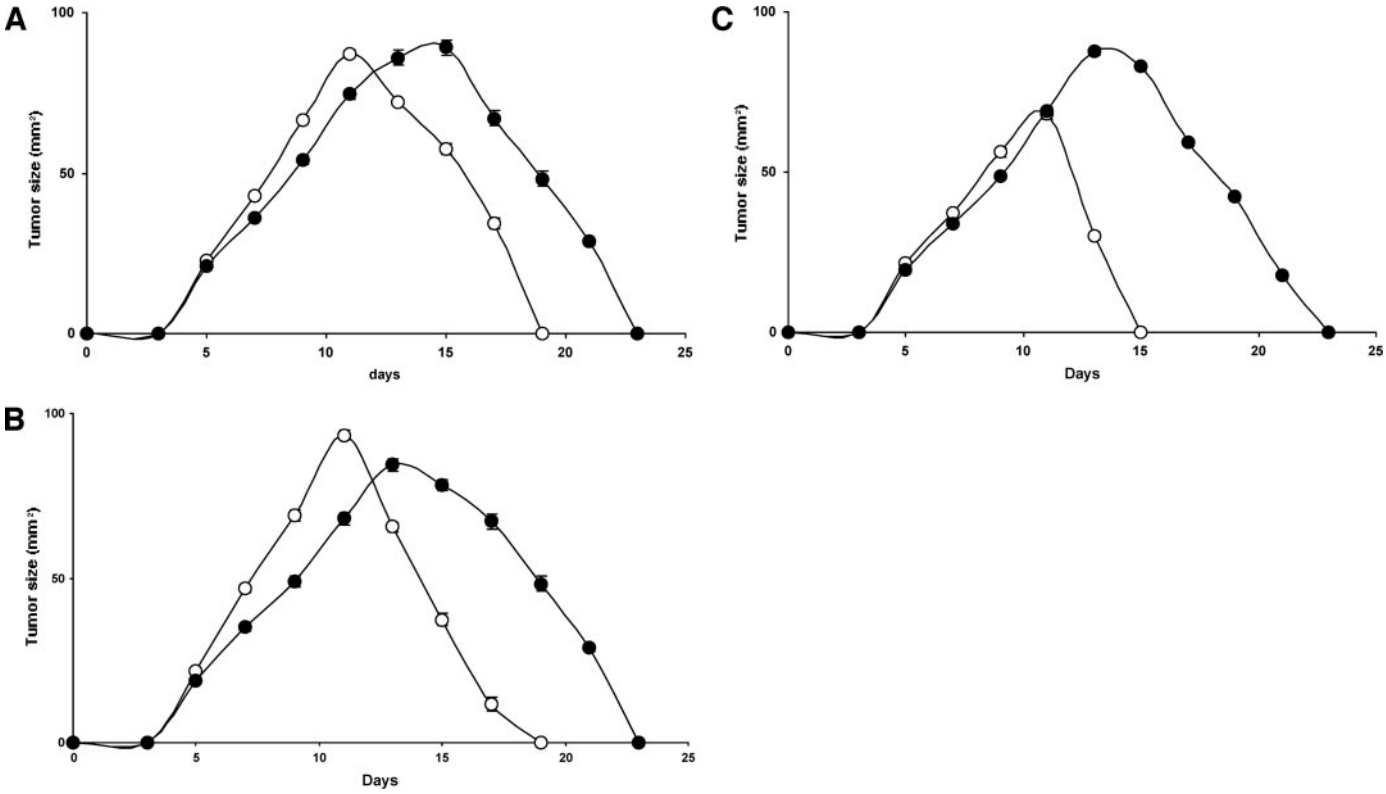

Fig. 6. Tumor regression is delayed by treatment with selective and nonselective nitric oxide synthase (NOS) inhibitors and by a NO scavenger. Mice were implanted with the recloned E.G7-OVA cell line that expressed relatively high levels of surface ovalbumin. Data points (*symbols*), the mean ± SE of the volumes reported as the product of the two largest perpendicular diameters. The error bars lie within the symbols. *A*, ●, animals were given the nonselective NOS inhibitor, *N*ω-nitro-L-arginine methyl ester (L-NAME), in their drinking water (2 g/liter) for 7 days before tumor implantation and throughout the period of tumor growth and subsequent regression ($n = 12$). ○, control animals ($n = 12$). *B*, ●, animals were given the inducible NOS (iNOS)-selective inhibitor, 1400W, which was administered via an osmotic minipump implanted s.c. at the same time as the tumor. The pump contained 50 mg of 1400W in 200 μl of PBS, which was delivered at a rate of 1.0 μl/h ($n = 6$). ○, control animals, in which the pump contained PBS alone ($n = 6$). *C*, ●, animals were treated with the NO scavenger $Ru(H_3dtpa)(Cl)$ for 14 days from the day of tumor implantation at a dose of 75 mg/kg administered i.p. twice daily ($n = 12$). ○, control animals received PBS alone ($n = 12$).

trichrome-stained sections of these tumors through the presence of condensed and fragmented nuclei. Although tumor-derived NO can be immunosuppressive (49) and, at low concentrations, it can also have antiapoptotic effects (4–6), at higher concentrations, it has been shown to promote tumor cell apoptosis (9–11). In E.G7-OVA tumors expressing relatively high levels of surface ovalbumin and treated with the nonspecific NOS inhibitor L-NAME, there was a reduction both in nitrotyrosine staining (see above) and in the number of apoptotic cells, implying that NO facilitates immune rejection of this tumor model by inducing tumor cell apoptosis. The number of apoptotic nuclei per high power field of view (×400, 10 fields counted) was 10.2 ± 0.7 in the control group *versus* 3.9 ± 0.8 in the group treated with L-NAME in the drinking water ($n = 10$ tumors; mean ± SD; $P < 0.01$). Previous studies have shown that cytokines secreted by activated immune cells can increase tumor cell NO synthesis and that this increase in NO production can induce tumor cell death by apoptosis (10). Therefore, we investigated whether cytokines secreted by activated immune cells could up-regulate NO synthesis in EL-4 cells and whether this could then result in their apoptosis.

Incubation of EL-4 cells with the NO donor, *S*-nitrosyl acetylpenicillamine, resulted in a time-dependent increase in the number of apoptotic cells and in the medium nitrite concentration (Fig. 8), demonstrating that the cells were sensitive to NO-induced apoptosis. EL-4 cells, cultured in conditioned medium that had been prepared by incubating splenocytes with irradiated E.G7-OVA cells, also showed increases in medium nitrite levels (Fig. 9*A*), NOS activity (Fig. 9*B*), and apoptosis (Fig. 9*C*). The splenocytes had been isolated from mice that had previously been implanted with E.G7-OVA cells expressing high levels of surface ovalbumin (see "Materials and Methods" section). The increase in nitrite levels and apoptosis were inhibited by the inclusion of L-NAME in the culture medium (Fig. 9, *A* and *C*).

DISCUSSION

The effect of NO on tumor growth is dependent on the concentrations that it reaches within the tissue, which will, in part, depend on the NOS isoform responsible for its production and on the cell-specific characteristics of the tumor cell itself, *e.g.*, p53 status (14, 15). There is a considerable body of evidence that, at relatively low concentrations, NO will promote tumor angiogenesis, stimulating the growth of primary tumors and promoting their subsequent metastasis (7, 8). NO has been shown to increase the expression of vascular endothelial growth factor (VEGF; Ref. 50), as well as acting as a downstream effector of VEGF action (51). The levels of NOS protein or activity have been positively correlated with the degree of malignancy in a number of human cancers, and there is evidence that NO produced by tumor-infiltrating macrophages can promote tumor angiogenesis (16, 52, 53). In contrast to the tumor-promoting effects of relatively low NO concentrations, higher concentrations have been shown to induce tumor cell apoptosis and to suppress tumor growth. NOS activity was inversely correlated with tumor growth and metastasis in a murine melanoma model (54), and engineered overexpression of iNOS was shown to reduce tumorigenicity through NO-mediated tumor cell death (15). The production of NO by activated macrophages and the resulting inhibition of tumor cell growth and/or

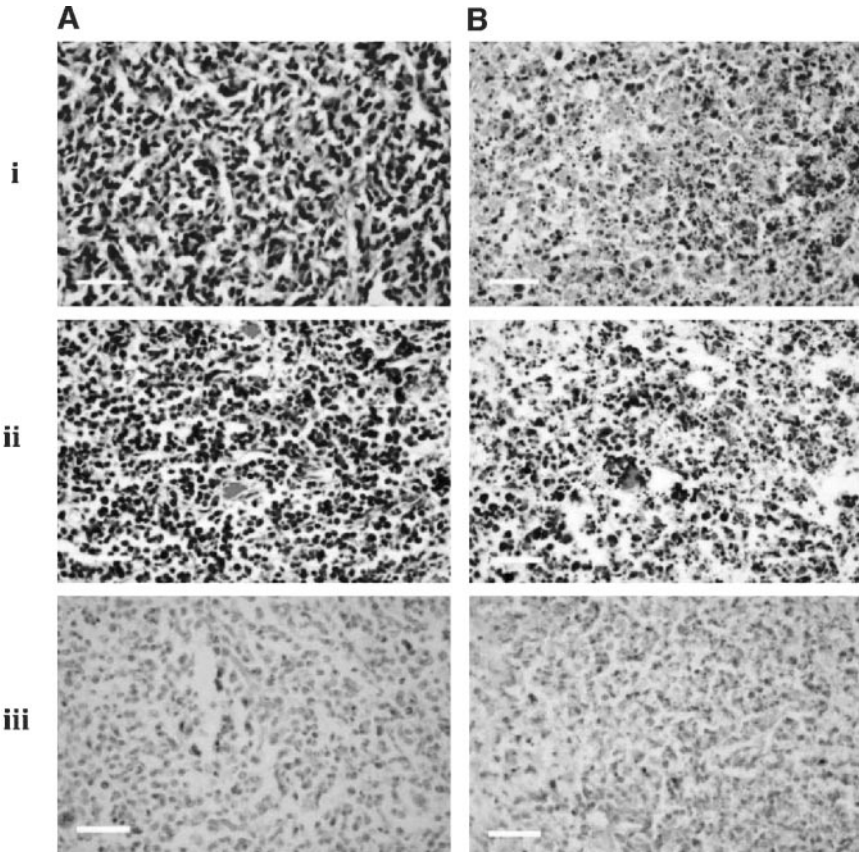

Fig. 7. Association of nitrotyrosine staining with the presence of apoptotic tumor cells in regressing E.G7-OVA tumors. Regressing tumors showed regions in which there were large numbers of apoptotic cells (*B*), and also regions that were relatively free of apoptosis (*A*). The presence of apoptotic tumor cells could readily be discerned through the presence of condensed and fragmented nuclei in sections stained with H&E (*i*) and with Masson's Trichrome stain (*ii*). These regions containing apoptotic cells also showed the presence of nitrated protein when adjacent sections were stained with a rabbit polyclonal antibody recognizing nitrated keyhole limpet hemocyanin and an appropriate secondary antibody (*iii*), as described in the "Materials and Methods" section. *Scale bars,* 150 μm.

induction of tumor cell apoptosis was the first function of NO in the immune system to be discovered (55). NO production by activated macrophages has been demonstrated to have tumoricidal activity *in vitro* (19–21); and, *in vivo*, tumor-mediated suppression of macrophage iNOS expression (24), deletion of the iNOS gene in the tumor host (25), and pharmacological inhibition of NO production (23) have all been shown to correlate with reduced or delayed tumor rejection. These studies imply a central role for macrophage-generated NO in tumor rejection. However, it is possible that tumor cell death can also result from induction of NOS activity in the tumor cells themselves. In a study of immune rejection of murine skin tumors, macrophage depletion of excised tumors could not completely reverse NO production, and it was suggested that cytokine-induced NO synthesis within the tumor cells themselves might also have contributed to their death and the consequent regression of the tumor (23). However, there seem to have been no studies that have demonstrated *in vivo* that induction of tumor NOS activity, during tumor rejection, can lead to tumor cell death and, thus, contribute to the rejection process.

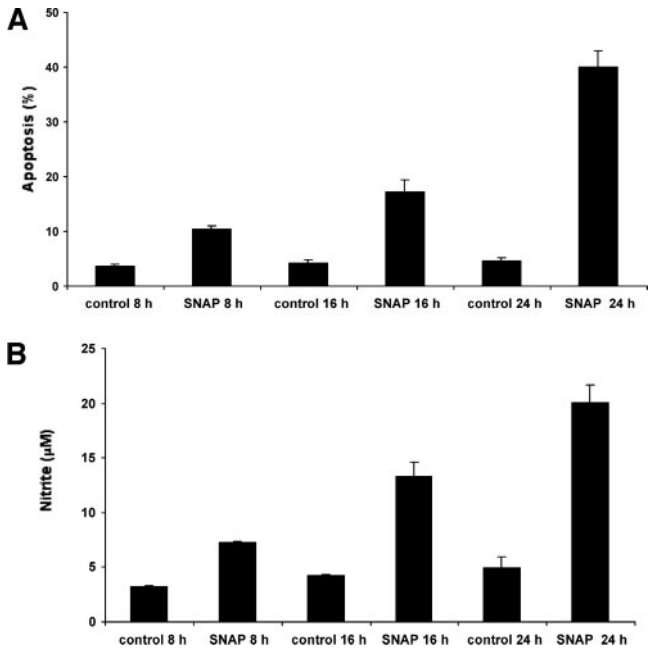

Fig. 8. The nitric oxide (NO) donor, *S*-nitrosyl acetylpenicillamine (*SNAP*), induced apoptosis in EL-4 cells. The cells were incubated at a density of 1×10^6 cells/ml with 1 mM SNAP, and medium nitrite levels were assessed using Griess reagent. Apoptosis was scored after staining of the cells with acridine orange and propidium iodide (see "Materials and Methods" section). The data represent the mean $\pm$ SE ($n = 4$). Apoptosis was significantly higher in the treated groups when compared with controls ($P < 0.01$).

A large range of tumor-specific antigens are expressed as neo-antigens throughout the progression of cancer, many of which are tumor specific or vary in their level of expression at different stages of the disease (56). We have used ovalbumin here as a model antigen to mimic the expression of neo-tumor antigens. The limitations of ovalbumin as a tumor antigen may be that the dose and context of presentation of antigenic epitopes to the immune system may be inappropriate and the response more vigorous than might be expected for low-level neo-antigen expression during the natural development of a tumor. However, by selecting E.G7-OVA cells with different levels of surface expression of ovalbumin, we have been able to titrate the immunogenicity of this tumor model. We have used this model to resolve the effects of host-derived NO in the growth and subsequent immune rejection of this murine lymphoma model by growing E.G7-OVA tumors, expressing different levels of surface ovalbumin, in mice in which the genes for iNOS or eNOS had been ablated. The role of tumor-derived NO was determined by using specific and nonspecific NOS inhibitors and a NO scavenger.

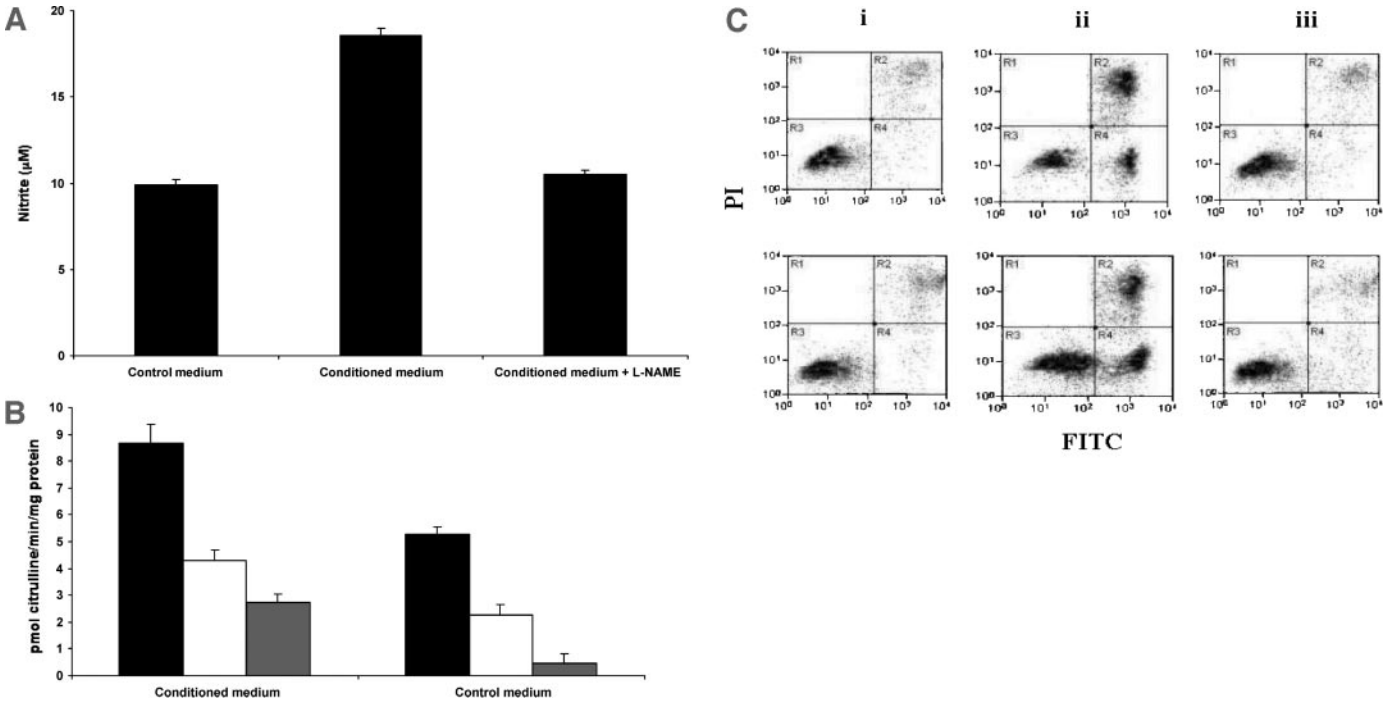

Fig. 9. Conditioned medium from activated splenocyte cultures increases nitric oxide synthase (NOS) activity and NO production and induces apoptosis in EL-4 cells. Preparation of conditioned medium and a conditioned medium control are described in the "Materials and Methods" section. *A*, EL-4 cells were incubated for 48 h with control or conditioned medium or conditioned medium plus 1 mM *N*ω-nitro-L-arginine methyl ester (*L-NAME*), and the levels of nitrite were determined using Griess reagent ($n = 6$; mean ± SE). Conditioned medium caused a significant increase in medium nitrite concentration ($P < 0.01$), which was significantly decreased by L-NAME ($P < 0.01$). *B*, NOS activity in cells treated for 48 h with control and conditioned medium. The activities shown were those obtained after subtraction of the activities measured in the absence of NADPH. ■, total NOS activity; □, NOS activity measured in the presence of the constitutive isoform of NOS (cNOS) inhibitor, W13 [*i.e.*, inducible NOS (iNOS) activity]; ▨, the activity measured in the presence of the iNOS inhibitor, 1400W (*i.e.*, cNOS activity). The activities shown are the mean ± SE ($n = 3$). The total NOS activity and the activities of iNOS and cNOS are significantly higher in EL-4 cells cultured in conditioned medium compared with those cultured in control medium ($P < 0.05$). *C*, apoptosis was assessed by flow cytometry after staining of the cells with FITC-labeled annexin V and propidium iodide (*PI*). Fluorescence emission was measured at 530 nm (FITC) and at >575 nm (PI). Viable cells show low levels of annexin-FITC and PI staining (*quadrant R3*); apoptotic cells stain with annexin-FITC (*quadrant R4*); necrotic cells stain with annexin-FITC and PI (*quadrant R2*). Cells were incubated for 48 h with control medium (*i*), with conditioned medium (*ii*), and with conditioned medium plus 1 mM L-NAME (*iii*). Apoptosis was significantly higher in the cells treated with conditioned medium (21.4 ± 1.4%, mean ± SE) when compared with cells incubated with control medium (4.4 ± 0.4%, mean ± SE; $P < 0.01$; $n = 7$). The level of apoptosis was decreased significantly by L-NAME (7.5 ± 1.5%, mean ± SE; $P < 0.01$; $n = 6$).

Host-derived NO seemed to have no effect on tumor angiogenesis because, as well as having no significant effect on tumor growth rate, host NOS status had no effect on the vascular volumes of growing tumors or on the increased vascularity observed in tumors undergoing immune rejection. We have shown previously that the increased vascularization observed in regressing E.G7-OVA tumors is accompanied by systemic and tumor increases in VEGF concentration (35). Inhibition of host and tumor NOS activities with an iNOS-selective inhibitor (1400W) and a nonselective inhibitor (L-NAME) appeared to slow the growth of E.G7-OVA cells expressing relatively high levels of ovalbumin, suggesting that tumor-derived NO might play a role in the growth of these tumors. However,. this effect was not statistically significant. Removal of NO with a scavenger also had no statistically significant effects on tumor growth rates.

Host-derived NO also appeared to have no effect on tumor immune rejection because rejection was unaffected by host NOS status. Rejection of these tumors has been shown previously to be accompanied by significant infiltration of $CD8^+$ T cells (32), and their migration away from the tumor was shown to result in continued tumor growth (57). However, the absence of any effect of host NOS status on tumor immune rejection cannot be explained by differences in immune cell infiltration, because the infiltration of $CD4^+$ and $CD8^+$ T cells and macrophages (CD68) were comparable in the wild-type and gene knock-out mice.

Although there was no evidence that host-derived NO was involved in the immune rejection of the EL-4-derived tumors used in this study, there was, nevertheless, clear evidence that NO played a role in the rejection process and that this NO must have come from the tumor cells. E.G7-OVA tumors had significantly higher levels of nitrite, an indicator of NO production, and protein nitration, which has been associated with the cellular damage caused by NO production (45), than nonexpressing tumors (EL-4), and these levels were further increased in regressing E.G7-OVA tumors. These levels, however, were unaffected by host NOS status. Measurements of tumor iNOS and constitutive isoforms of NOS activities in the iNOS and eNOS knockout mice showed that much of the NOS activity in the tumor must have come from the tumor cells themselves. Inhibiting tumor NOS activity with a nonselective NOS inhibitor (L-NAME), or an iNOS-selective inhibitor (1400W), or scavenging NO with a ruthenium-based NO scavenger, delayed significantly the rejection of those E.G7-OVA tumors that expressed relatively high levels of surface ovalbumin. In those tumors that had been treated with L-NAME, there was a significant reduction in protein nitration and in the levels of associated apoptotic tumor cells.

The mechanisms by which NO induces apoptosis are still poorly characterized (58). There is evidence that induction of apoptosis by NO requires the production of ROS (58). The observation of nitrotyrosine in the regressing E.G7-OVA tumors indicates the presence of both NO and ROS (46). Whether these ROS also come from the tumor cells, or from infiltrating macrophages, is not clear. In the B16 melanoma tumor model, vaccination-induced tumor rejection was reduced significantly in mice with a defective NADPH oxidase enzyme-complex, indicating that, in this case, the ROS came mainly from host cells in the tumor (25). However, the role of host NOS

activity in the growth, vascularization, and immune rejection of this melanoma seem to be in direct contrast with the results obtained here on the EL-4 lymphoma. In the B16 melanoma, disruption of the host iNOS gene inhibited the growth of the primary tumor (59), inhibited metastasis (60), impaired tumor-induced angiogenesis in lung metastases (61), reduced tumor VEGF levels (59, 61), and reduced significantly (by 40–50%) vaccination-induced immune rejection (25). This tumor, unlike the EL-4 lymphoma used here, was assumed not to express iNOS because no iNOS mRNA could be detected in lung metastases from iNOS knockout mice and no iNOS protein could be detected in cells incubated with IFN-γ and LPS, conditions known to induce iNOS activity in most murine tumor cells (61). However, in a subsequent study, iNOS immunoreactivity was identified in B16 melanoma cells growing in wild-type mice but not in iNOS knockout mice, implying that iNOS induction in the B16 melanoma is dependent on iNOS expression in the host (59). The reasons for this are not clear; however, this observation raises the possibility that the vaccination-induced immune rejection of B16 tumors that was observed previously (25) and that was inhibited in iNOS knockout mice might also depend on induction of tumor iNOS activity, as was observed here for the EL-4 lymphoma.

A factor which might contribute to differences in the growth and immune rejection of the EL-4 lymphoma and the B16 melanoma is their relative sensitivity to the toxic effects of NO. The B16 melanoma seems to be significantly less sensitive than the EL-4 lymphoma. After incubation with *S*-nitrosyl acetylpenicillamine at a concentration of 0.8 mM for 24 h, there was $<$10% cytotoxicity in B16 melanoma cells, as judged by a 3-(4,5-dimethylthiazol-2-yl)-2,5-diphenyltetrazolium bromide reduction assay (60), whereas incubation of the EL-4 lymphoma cells, in this study, with 1 mM *S*-nitrosyl acetylpenicillamine for 24 h resulted in $\sim$40% apoptosis. This might help to explain why induction of tumor iNOS activity, which in the B16 melanoma leads to increased VEGF production and promotes tumor growth (59), in the EL-4 lymphoma resulted in tumor cell apoptosis. However, there is clearly also a difference in the nature of the immune response to these two tumor types. Vaccination of B16 melanoma-bearing mice with irradiated tumor cells expressing granulocyte/macrophage colony-stimulating factor resulted in significant infiltration of macrophages that stained strongly positive for iNOS. The protection offered by vaccination against subsequent challenge with the tumor was reduced substantially in iNOS knockout mice (25). This is in contrast to what was observed here with the EL-4 lymphoma, in which, despite macrophage infiltration, there was no evidence of significant macrophage NOS activity, and deletion of the host iNOS gene had no effect on tumor immune rejection.

Previous work has shown that *in vitro*, IFN-γ and tumor necrosis factor α, secreted by cytotoxic lymphocytes, can induce iNOS activity in human colon cancer cells and that the resulting increase in NO production induces tumor cell apoptosis (10). We have shown here that incubation of tumor cells with medium taken from activated splenocyte cultures resulted in increased tumor cell NOS activity, the accumulation of nitrite in the culture medium, and apoptosis of the tumor cells. Furthermore .the accumulation of nitrite and the increase in apoptosis could be inhibited by inhibition of NOS activity with L-NAME. We propose, therefore, that during the immune rejection of this tumor model, there is induction of tumor NOS activity by cytokines secreted by activated lymphocytes within the tumor and that this results in increased levels of tumor NO that induce tumor cell apoptosis. This NO-induced tumor cell apoptosis seems to facilitate immune rejection of the tumor, as inhibition of tumor NO production *in vivo* delayed tumor rejection. Because the induction of NO synthesis in response to cytokines secreted by activated lymphocytes has been demonstrated in a number of human tumor cell lines (see references cited in Ref. 10), this may be an important mechanism involved in the immune rejection of this and other tumor types.

ACKNOWLEDGMENTS

We thank Salvador Moncada for his advice and encouragement, Guy Brown for his assistance with the NO electrode measurements, and Jonathan Schmitz for his help with the flow cytometry.

REFERENCES

1. Moncada, S., Palmer, R. M. J., and Higgs, E. A. Nitric oxide: physiology, pathophysiology, and pharmacology. Pharmacol. Rev., *43:* 109–142, 1991.
2. Knowles, R. G., and Moncada, S. Nitric oxide synthase in mammals Biochem. J., *298:* 249–258, 1994.
3. Elfering, S. L., Sarkela, T. M., and Giulivi, C. Biochemistry of mitochondrial nitric-oxide synthase. J. Biol. Chem., *277:* 38079–38086, 2002.
4. Zhao, H., Dugas, N., Mathiot, C., Delmer, A., Dugas, B., Sigaux, F., and Kolb, J-P. B-cell chronic lymphocytic leukemia cells express a functional inducible nitric oxide synthase displaying anti-apoptotic activity. Blood, *92:* 1031–1043, 1998.
5. Mannick, J. B., Miao, X. Q., and Stamler, J. S. Nitric oxide inhibits Fas-induced apoptosis. J. Biol. Chem., *272:* 24125–24128, 1997.
6. Arnold, R. E., and Weigent, D. A. The production of nitric oxide in EL4 lymphoma cells overexpressing growth hormone. J. Neuroimmunol., *134:* 82–94, 2003.
7. Fukumura, D., and Jain, R. K. Role of nitric oxide in angiogenesis and microcirculation in tumors. Cancer Metastasis Rev., *17:* 77–89, 1998.
8. Carmeliet, P., and Jain, R. K. Angiogenesis in cancer and other diseases. Nature (Lond.), *407:* 249–257, 2000.
9. Xie, K., and Fidler, I. J. Therapy of cancer metastasis by activation of the inducible nitric oxide synthase. Cancer Metastasis Rev., *17:* 55–75, 1998.
10. Kwak, J-Y., Han, M. K., Choi, K-S., Park, I-H., Park, S-Y., Sohn, M-H., Kim, U-H., McGregor, J. R., Samlowski, W. E., and Yim, C-Y. Cytokines secreted by lymphokine-activated killer cells induce endogenous nitric oxide synthesis and apoptosis in DLD-1 colon cancer cells. Cell. Immunol., *203:* 84–94, 2000.
11. Lee, V. Y., McClintock, D. S., Santore, M. T., Budinger, G. R. S., and Chandel, N. S. Hypoxia sensitizes cells to nitric oxide-induced apoptosis. J. Biol. Chem., *277:* 16067–16074, 2002.
12. Jenkins, D. C., Charles, I. G., Thomsen, L. L., Moss, D. W., Holmes, L. S., Baylis, S. A., Rhodes, P., Westmore, K., Emson, P. C., and Moncada, S. Roles of nitric oxide in tumor growth. Proc. Natl. Acad. Sci. USA, *92:* 4392–4396, 1995.
13. Xie, K., Huang, S., Dong, Z., Juang, S-H., Gutman, M., Xie, Q-W., Nathan, C., and Fidler, I. J. Transfection with the inducible nitric oxide synthase gene suppresses tumorigenicity and abrogates metastasis by K-1735 murine melanoma cells. J. Exp. Med., *181:* 1333–1343, 1995.
14. Ambs, S., Merriam, W. G., Ogunfusika, M. O., Bennett, W. P., Ishibe, N., Hussain, S. P., Tzeng, E. E., Geller, D. A., Billiar, T. R., and Harris, C. C. p53 and vascular endothelial growth factor regulate tumor growth of NOS2-expressing human carcinoma cells. Nat. Med., *4:* 1371–1376, 1998.
15. Shi, Q., Huang, S., Jiang, W., Kutach, L. S., Ananthaswamy, H. N., and Xie, K. Direct correlation between nitric oxide synthase II inducibility and metastatic ability of UV-2237 murine fibrosarcoma cells carrying mutant p53. Cancer Res., *59:* 2072–2075, 1999.
16. Thomsen, L., and Miles, D. W. Role of nitric oxide in tumour progression: lessons from human tumours. Cancer Metastasis Rev., *17:* 107–118, 1998.
17. Leek, R. D., Lewis, C. E., Whitehouse, R., Greenall, M., Clarke, J., and Harris, A. L. Association of macrophage infiltration with angiogenesis and prognosis in invasive breast cancer. Cancer Res., *56:* 4625–4629, 1996.
18. Leek, R. D., Lewis, C. E., and Harris, A. L. The role of macrophages in tumour angiogenesis. *In:* R. Bicknell, C. E. Lewis, and N. Ferrara (eds.), Tumour Angiogenesis, pp. 81–99. Oxford, England: Oxford University Press, 1997.
19. Stuehr, D. J., and Nathan, C. F. Nitric oxide. A macrophage product responsible for cytostasis and respiratory inhibition in tumor target cells, J. Exp. Med., *169:* 1543–1555, 1989.
20. Keller, R., Geiges, M., and Keist, R. L-arginine-dependent reactive nitrogen intermediates as mediators of tumor cell killing by activated macrophages. Cancer Res., *50:* 1421–1425, 1990.
21. Cui, S., Reichner, J. S., Mateo, R. B., and Albina, J. E. Activated murine macrophages induce apoptosis in tumor cells through nitric oxide-dependent or -independent mechanisms. Cancer Res., *54:* 2462–2467, 1994.
22. Ambs, S., Merriam, W. G., Bennett, W. P., Felley-Bosco, E., Ogunfusika, M. O., Oser, S. M., Klein, S., Shields, P. G., Billiar, T. R., and Harris, C. C. Frequent nitric oxide synthase-2 expression in human colon adenomas: implication for tumor angiogenesis and colon cancer progression. Cancer Res., *58:* 334–341, 1998.
23. Yim, C. Y., Bastian, N. R., Smith, J. C., Hibbs, J. B., and Samlowski, W. E. Macrophage nitric oxide synthesis delays progression of ultraviolet light-induced murine skin cancers. Cancer Res., *53:* 5507–5511, 1993.
24. Dinapoli, M. R., Calderon, C. L., and Lopez, D. M. The altered tumoricidal capacity of macrophages isolated from tumor-bearing mice is related to reduced expression of the inducible nitric oxide synthase gene. J. Exp. Med., *183:* 1323–1329, 1996.
25. Hung, K., Hayashi, R., Lafond-Walker, A., Lowenstein, C., Pardoll, D., and Levitsky, H. The central role of $CD4^+$ T cells in the antitumor immune response. J. Exp. Med., *188:* 2357–2368, 1998.

26. Amber, I. J., Hibbs, J. B. J., Taintor, R. R., and Vavrin, Z. The L-arginine dependent effector mechanism is induced in murine adenocarcinoma cells by culture supernatant from cytotoxic activated macrophages. J. Leukocyte Biol., *43:* 187–192, 1988.
27. Moore, M. W., Carbone, F. R., and Bevan, M. J. Introduction of soluble protein into the class I pathway of antigen processing and presentation. Cell, *54:* 777–785, 1988.
28. Laubach, V. E., Shesely, E. G., Smithies, O., and Sherman, P. A. Mice lacking inducible nitric oxide synthase are not resistant to lipopolysaccharide-induced death, Proc. Natl. Acad. Sci. USA, *92:* 10688–10692, 1995.
29. Huang, P. L., Huang, Z., Mashimo, H., Bloch, K. D., Moskowitz, M. A., Bevan, J. A., and Fishman, M. C. Hypertension in mice lacking the gene for endothelial nitric oxide synthase. Nature (Lond.), *377:* 239–242, 1995.
30. Mosi, R., Seguin, B., Cameron, B., Amankwa, L., Darkes, M. C., and Fricker, S. P. Mechanistic studies on AMD6221: a ruthenium-based nitric oxide scavenger, Biochem. Biophys. Res. Commun., *292:* 519–529, 2002.
31. Sandhu, J. K., Privora, H. F., Wenckebach, G., and Birnboim, H. C. Neutrophils, nitric oxide synthase, and mutations in the mutatect murine tumor model. Am. J. Pathol., *156:* 509–518, 2000.
32. Dyall, R., Vasovic, L. V., Clynes, R. A., and Nikolic-Zugic, J. Cellular requirements for the monoclonal antibody-mediated eradication of an established solid tumour. Eur. J. Immunol., *29:* 30–37, 1999.
33. Mayhew, T. M., and Sharma, A. K. Sampling schemes for estimating nerve-fiber size. II. Methods for nerve trunks of mixed fascicularity, J. Anat., *139:* 45–58, 1984.
34. Kimura, M., Amemiya, K., Yamada, T., and Suzuki, J. Quantitative method for measuring adjuvant-induced granuloma angiogenesis in insulin-treated diabetic mice. J. Pharmacobio-Dyn., *9:* 442–446, 1986.
35. Hu, D-E., Beauregard, D. A., Bearchell, M. C., Thomsen, L. L., and Brindle, K. M. Early detection of tumour immune-rejection using magnetic resonance imaging. Br. J. Cancer, *88:* 1135–1142, 2003.
36. Misko, T. P., Schilling, R. J., Salvemini, D., Moore, W. M., and Currie, M. G. A fluorometric assay for measurement of nitrite in biological samples. Anal. Biochem., *214:* 11–16, 1993.
37. Ju, D. W., Tao, Q., Lou, G., Bai, M., He, L., Yang, Y., and Cao, X. Interleukin 18 transfection enhances anti-tumor immunity induced by dendritic cell-tumor cell conjugates. Cancer Res., *61:* 3735–3740, 2001.
38. Ke, Y., Ma, H., and Kapp, J. A. Antigen is required for the activation of effector activities, whereas interleukin 2 is required for the maintenance of memory in ovalbumin-specific, CD8+ cytotoxic T lymphocytes. J. Exp. Med., *187:* 49–57, 1998.
39. Anthony, M. L., Zhao, M., and Brindle, K. M. Inhibition of phosphatidylcholine biosynthesis following induction of apoptosis in HL-60 cells. J. Biol. Chem., *274:* 19686–19692, 1999.
40. Brossart, P., Goldrath, A. W., Butz, E. A., Martin, S., and Bevan, M. J. Virus-mediated delivery of antigenic epitopes into dendritic cells as a means to induce CTL. J. Immunol., *158:* 3270–3276, 1997.
41. Vasovic, L. V., Dyall, R., Clynes, R. A., Ravetch, J. V., and Nikolic-Zugic, J. Synergy between an antibody and CD8(+) cells in eliminating an established tumor. Eur. J. Immunol., *27:* 374–382, 1997.
42. Minev, B. R., McFarland, B. J., Spiess, P. J., Rosenberg, S. A., and Restifo, N. P. Insertion signal sequence fused to minimal peptides elicits specific Cd8+ T-cell responses and prolongs survival of thymoma-bearing mice. Cancer Res., *54:* 4155–4161, 1994.
43. Zhou, F., Rouse, B. T., and Huang, L. Prolonged survival of thymoma-bearing mice after vaccination with a soluble-protein antigen entrapped in liposomes: a model study. Cancer Res., *52:* 6287–6291, 1992.
44. Ramprasad, M. P., Fischer, W., Witztum, J. L., Sambrano, G. R., Quehenberger, O., and Steinberg, D. The 94-Kda to 97-Kda mouse macrophage membrane-protein that recognizes oxidized low-density-lipoprotein and phosphatidylserine-rich liposomes is identical to macrosialin, the mouse homolog of human Cd68. Proc. Natl. Acad. Sci. USA, *92:* 9580–9584, 1995.
45. Gal, A., Tamir, S., Kennedy, L. J., Tannenbaum, S. R., and Wogan, G. N. Nitrotyrosine formation, apoptosis, and oxidative damage: relationships to nitric oxide production in SJL mice bearing the RcsX tumor. Cancer Res., *57:* 1823–1828, 1997.
46. Ischiropoulos, H. Biological tyrosine nitration: a pathophysiological function of nitric oxide and reactive oxygen species. Arch. Biochem. Biophys., *356:* 1–11, 1998.
47. Thomsen, L. L., Scott, J. M. J., Topley, P., Knowles, R. G., Keerie, A-J., and Frend, A. J. Selective inhibition of inducible nitric oxide synthase inhibits tumor growth *in vivo*: studies with 1400W, a novel inhibitor. Cancer Res., *57:* 3300–3304, 1997.
48. Pieper, G. M., Roza, A. M., Adams, M. B., Hilton, G., Johnson, M., Felix, C. C., Kampalath, B., Darkes, M., Wanggui, Y., Cameron, B., and Fricker, S. P. A ruthenium (III) polyaminocarboxylate complex, a novel nitric oxide scavenger, enhances graft survival and decreases nitrosylated heme protein in models of acute and delayed cardiac transplant rejection, J. Cardiovasc. Pharmacol., *39:* 441–448, 2002.
49. Nathan, C. Nitric oxide as a secretory product of mammalian cells. FASEB J., *6:* 3051–3064, 1992.
50. Chin, K., Kurashima, Y., Ogura, T., Tajiri, H., Yoshida, S., and Esumi, H. Induction of vascular endothelial growth factor by nitric oxide in human glioblastoma and hepatocellular carcinoma cells. Oncogene, *15:* 437–442, 1997.
51. Ziche, M., Morbidelli, L., Choudhuri, R., Zhang, H-T., Donnini, S., Granger, H. J., and Bicknell, R. Nitric oxide synthase lies downstream from vascular endothelial growth factor-induced but not basic fibroblast growth factor-induced angiogenesis. J. Clin. Investig., *99:* 2625–2634, 1997.
52. Thomsen, L. L., Miles, D. W., Happerfield, L., Bobrow, L. G., Knowles, R. G., and Moncada, S. Nitric oxide synthase activity in human breast cancer. Br. J. Cancer, *72:* 41–44, 1995.
53. Thomsen, L. L., Lawton, F. G., Knowles, R. G., Beesley, J. E., Riveros-Moreno, V., and Moncada, S. Nitric oxide synthase activity in human gynecological cancer. Cancer Res., *54:* 1352–1354, 1994.
54. Dong, Z., Staroselsky, A. H., Qi, X., Xie, K., and Fidler, I. J. Inverse correlation between expression of inducible nitric oxide synthase activity and production of metastasis in K-1735 murine melanoma cells. Cancer Res., *54:* 789–793, 1994.
55. Bogdan, C. Nitric oxide and the immune response. Nat. Immunol., *2:* 907–916, 2001.
56. Rosenberg, S. A. Progress in human tumour immunology and immunotherapy. Nature (Lond.), *411:* 380–384, 2001.
57. Shrikant, P., and Mescher, M. F. Control of syngeneic tumor growth by activation of CD8+ T cells: efficacy is limited by migration away from the site and induction of nonresponsiveness. J. Immunol., *162:* 2858–2866, 1999.
58. Brown, G. C., and Borutaite, V. Nitric oxide inhibition of mitochondrial respiration and its role in cell death. Free Radic. Biol. Med., *26:* 925–935, 2002.
59. Konopka, T. E., Barker, J. E., Bamford, T. L., Guida, E., Anderson, R. L., and Stewart, A. G. *Nitric oxide synthase II* gene disruption: implications for tumor growth and vascular endothelial growth factor production. Cancer Res., *61:* 3182–3187, 2001.
60. Shi, Q., Xiong, Q., Wang, B., Le, X., Khan, N. A., and Xie, K. Influence of *nitric oxide synthase II* gene disruption on tumor growth and metastasis. Cancer Res., *60:* 2579–2583, 2000.
61. Wang, B., Xiong, Q., Shi, Q., Tan, D., Le, X., and Xie, K. Genetic disruption of host *nitrix oxide synthase II* gene impairs melanoma-induced angiogenesis and suppresses pleural effusion. Int. J. Cancer, *91:* 607–611, 2001.